DALTON PERSPECTIVE

Applications of advanced experimental techniques: high pressure NMR and computer simulations †

Lothar Helm and André E. Merbach

Institut de chimie moléculaire et biologique, Ecole polytechnique fédérale de Lausanne, CH-1015 Lausanne, Switzerland. E-mail: Lothar.Helm@epfl.ch; Andre.Merbach@epfl.ch

Received 13th September 2001, Accepted 24th October 2001
First published as an Advance Article on the web 18th January 2002

The usefulness of pressure variation for the elucidation of mechanisms of solvent exchange reactions on metal ions is discussed. Even if the distinction between a limiting and an interchange mechanism, based on the magnitude of the activation volumes, is not straightforward, the activation mode, associative or dissociative, can be assigned from the sign of $\Delta V^{\ddagger}$. The use of quantum mechanical calculations has also become a valuable tool in studies of exchange reactions. These calculations can be performed on the ground state and on transition states or intermediates with increased or decreased coordination number. They are useful for distinguishing between possible pathways and/or to give insight on the mechanism, not available experimentally.

† Based on the presentation given at Dalton Discussion No. 4, 10–13th January 2002, Kloster Banz, Germany.

Introduction

The substitution reaction on metal ions M may, in a general way, be written as:

$$L_nMX + Y \longrightarrow L_nMY + X \qquad (1)$$

To elucidate the mechanisms of such reactions, it is usual to measure the reaction rate as a function of a number of chemical (concentrations, pH, ionic strength, solvent) and physical (normally temperature) parameters. The empirical rate law, the electronic and steric effects induced by variations of leaving X, entering Y, and non-reacting L ligands, the variable temperature activation parameters (activation enthalpy, $\Delta H^{\ddagger}$ and activation entropy, $\Delta S^{\ddagger}$) and any other experimental or theoretical information available on the system are then used to assign a reaction mechanism. It is found however, that such information

Lothar Helm was born in 1952 in Gernsbach, Germany. He studied physics at the Technical University of Karlsruhe (Germany) and obtained his diploma in 1977. He remained in Karlsruhe for his Ph.D. research with Prof. H. G. Hertz and received his degree in physical chemistry in 1980. In 1980 he joined the laboratories of Prof. André Merbach at the University of Lausanne, Switzerland. From 1983 to 2001 he was maître d'enseignement et de recherche at the Faculty of Science of the University of Lausanne. In 2001 he moved, together with the whole chemistry department, from the University of Lausanne to the Swiss Federal Institute of Technology in Lausanne (EPFL). His main research interest is in the study of reaction mechanisms in coordination chemistry using multinuclear and high pressure NMR and computer simulation techniques.

Originating from Pully (Switzerland), André E. Merbach was born in 1940. He studied at the Polytechnical School of the University of Lausanne and obtained a degree in Chemical Engineering in 1962. In 1964, he was awarded his PhD in inorganic chemistry from the University of Lausanne. He then had a Postdoctoral Fellowship in the Lawrence Radiation Laboratory at the University of California, Berkeley, where he studied the ionisation of strong electrolytes by NMR. Upon his return, in 1965, to the Institute of Inorganic and Analytical Chemistry at the University of Lausanne, he accepted a teaching and research position in Coordination Chemistry. In 1973, the Swiss Chemical Society awarded him the Werner Prize and Medal for his work on the structure, the stability and the dynamics of metal halogen adducts by NMR and he was nominated Professor in Inorganic and Analytical Chemistry. He was a member of the Research Council of the NSF (1985–1996) and has chaired the European Technical Committee (COST) for chemical research (1998–2000). He organised the XXIXth International Conference in Coordination Chemistry (ICCC) in Lausanne in 1992. He was awarded an honorary doctorate (Honoris Causa) from the University of Lajos Kossuth in Debrecen (Hungary) in 1993 for his work on elucidating reaction mechanisms in coordination chemistry utilising high pressure NMR. Recently he has been elected President of the Swiss Chemical Society (2001–2004).

Lothar Helm

André Merbach

DOI: 10.1039/b108321j

may be insufficient to distinguish clearly between reaction mechanisms. This is especially so for an important class of substitution reactions in inorganic chemistry, namely solvent exchange reactions, where X = Y in eqn. (1). Normally one cannot vary the concentrations of the reactants (unless working with an 'inert' diluent) so that the mechanistic assignment must often be made on the basis of activation parameters alone.

Fortunately, temperature is not the only physical variable which can be varied in kinetic studies. Pressure can also affect the rate of a substitution reaction in solution, and variable pressure measurements yield an activation volume, $\Delta V^{\ddagger}$, which can be used as a supplementary (and often decisive) parameter for mechanistic assignment.[1] Although the first high pressure kinetic study in inorganic chemistry was made over forty years ago,[2] the rapid development of the field has occurred in the last twenty years, since the adaptation for variable pressure studies of most fast reaction techniques: stopped-flow,[3] temperature-jump,[4] pressure-jump[5] and NMR.[6]

In recent years the application of classical molecular dynamics (MD) computer simulations as well as *ab-initio* and density functional (DFT) calculations have gained significant interest. Classical MD simulations of hydrated metal ions in solution mainly rely on pairwise additive, effective interaction potentials obtained from quantum mechanical calculations or from empirical optimization of thermodynamic values like hydration energies or radial distribution functions. This approach limits these simulations to metal ions with filled atomic orbitals, mainly to main group ions and those transition metal ions, where ligand field effects can be neglected (*e.g.* lanthanides). The advantage of the classical methods is that relatively large systems, containing up to 10^3 water molecules can be simulated over several ns (10^{-9} s). Exchange processes can be followed directly by inspecting trajectories, molecular coordinates and velocities as a function of time.

Full quantum mechanical calculations are computationally much more demanding and, therefore, mostly restricted to small ion–water clusters containing one metal ion and a limited number of water or other solvent molecules. Different metal–water clusters that can occur along the reaction coordinate of a water exchange process have to be calculated. A comparison of energies and structural parameters like metal–oxygen bond distances in the reactants, transition states and intermediates will help to associate them to different reaction mechanisms. In gas-phase calculations, second coordination sphere, bulk solvent and anions are neglected and, furthermore, contrary to classical molecular dynamics simulations no real timescale is provided. These calculations are not based on empirical pair wise additive interaction potentials and therefore calculations on all types of ions, including transition metals, are feasible.

A promising method, developed in the last decade, is first principles molecular dynamics like the Car–Parrinello technique.[7] In these calculations interatomic potentials are explicitly derived from electronic ground-state within the density functional theory in local or non-local approximation. It combines quantum mechanical calculations with molecular dynamics simulations and, therefore, overcomes the limitations of both methods. Actual computers allow only simulations of aqueous solutions of about 60 water molecules for a few ps (10^{-12} s). This limit is still at least one order of magnitude shorter than the fastest directly measured water exchange rate. Nevertheless, several publications appeared in the late nineties on solvated Be^{2+},[8] K^+ and Cu^{2+}[10] presenting mainly structural results.

Solvent exchange reactions: theoretical concept

The mechanistic classification accepted for ligand substitution reactions was proposed by Langford and Gray in 1965.[11] They divided substitution reactions into three categories of stoichiometric mechanisms: associative (A), where an intermediate of increased coordination number can be detected, dissociative (D) where an intermediate of reduced coordination number can be detected, and interchange (I) where there is no kinetically detectable intermediate. Furthermore, they distinguished two major categories of intimate mechanisms: those with an associative activation mode (a), where the reaction rate is approximately as sensitive (or more sensitive) to variation of the entering group as to variation of the leaving group, and those with a dissociative mode (d), where the reaction rate is much more sensitive to the variation of the leaving group than to the variation of the entering group. Evidently all D mechanisms must be dissociatively and all A mechanisms must be associatively activated. The I mechanisms include a continuous spectrum of transition states where the degree of bond-making between the incoming ligand and the complex ranges from very substantial (I_a mechanism) to negligible (I_d mechanism).[12] For a solvent exchange process, the forward and backward reaction coordinates must be symmetrical. Thus, for an I_d mechanism, with negligible bond-making of the entering group, the leaving group is also necessarily weakly bound. Inversely, for an I_a mechanism, both the entering and the leaving group must have a considerable bonding to the metal (Fig. 1).[12] Swaddle suggests

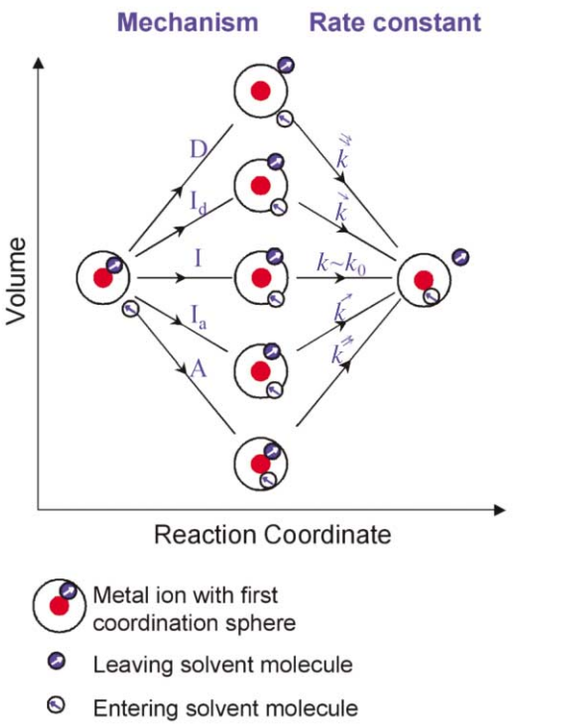

Fig. 1 Representation of the transition state for the spectrum of solvent or symmetrical ligand exchange processes.

that for substitution of solvents such as water on octahedral complexes, only I mechanisms need to be considered.[13] He assumes that associative A processes are sterically inhibited, whereas dissociative D mechanisms are unlikely due to the long life-times required for intermediates with a reduced coordination number (nanosecond time-scale). Furthermore, he concluded from early computer simulations[14] that there can be no clear-cut mechanistic classification of the I_a : I_d type[13] and proposed that there is just one interchange mechanism which spans an essentially infinite number of microscopic pathways. For a particular reaction a broad manifold of microscopic pathways will be more important than others, leading to a distinctive set of measurable parameters.

As mentioned above, the proposition of a reaction mechanism is based mainly on the response of the reaction rate to the variation of chemical and physical parameters. The volume of activation, $\Delta V^{\ddagger}$, has become the main tool for the experimental identification of the water exchange mechanism.[15] $\Delta V^{\ddagger}$

is defined as the difference between the partial molar volume of the reactants and that of the transition state at a temperature T, and given in eqn. (2).

$$\left(\frac{\partial \ln(k)}{\partial P}\right)_T = -\frac{\Delta V^{\ddagger}}{RT} \qquad (2)$$

The observed exchange rate constant, k, is either slowed or accelerated by increasing pressure, depending on the positive or negative sign of $\Delta V^{\ddagger}$, respectively. It is usually accepted that the activation volume has two contributions: an intrinsic component, $\Delta V_{int}^{\ddagger}$, resulting from changes in bond lengths and bond angles, and an electrostrictive component, $\Delta V_{elec}^{\ddagger}$, which arises from changes in electrostriction of the solvent outside the first coordination sphere. For solvent exchange reactions differences in electrostriction between the transition state and the reactant can be neglected, hence $\Delta V^{\ddagger} \approx \Delta V_{int}^{\ddagger}$. Consequently, the activation volume will be a direct measure of the degree of bond formation or bond breaking in the transition state (after correction of small volume changes due to the adjustment of the bond lengths of the spectator ligands at the transition state). The relation between the pressure induced changes of the observed exchange rates and the underlying solvent exchange reaction mechanisms is visualized in Fig. 1. An important issue is the prediction of activation volumes for the limiting substitution mechanisms D and A. Swaddle[16] developed a semi-empirical model in which the absolute partial molar volume, ΔV_{abs}^{0}, of a hydrated metal ion in water is related to its ionic radius, depending on the coordination number, and the charge of the metal ion. Taking ionic radii from Shannon,[17] this model gives similar absolute limiting values of $|\Delta V^{\ddagger}| = 13.5$ cm^3 mol^{-1} for D and A processes for water exchange on di-and tri-valent 3d transition metal ions.

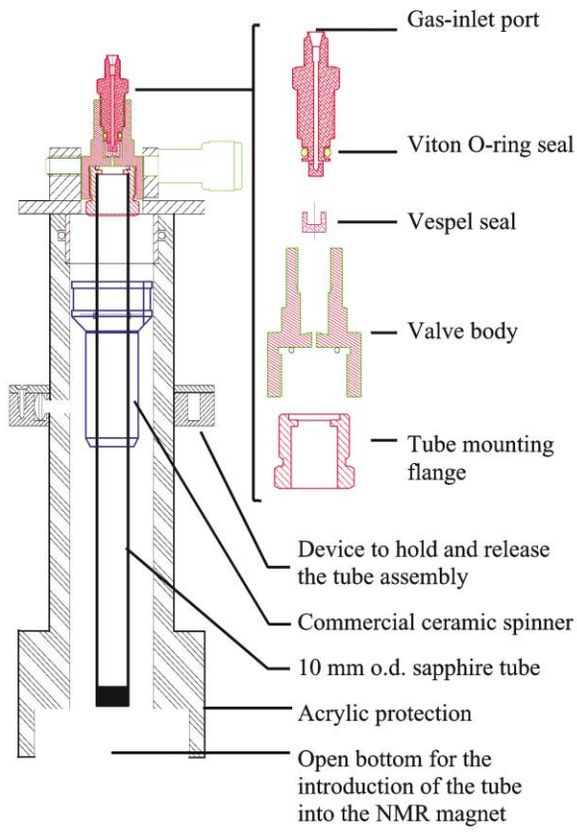

Fig. 2 Schematic drawing of the sapphire tube/Ti-valve assembly (expanded) and the safety device.

Variable pressure NMR

Since the pioneering work of Benedek and Purcell in the fifties[18] two general approaches have emerged for the measurement of high resolution NMR spectra at variable pressure.[19] One relatively simple approach consists of using a thick-walled glass container or a sapphire tube which can be placed directly into a standard NMR probe. An alternative approach is to build a dedicated high pressure NMR probe which will replace the ambient pressure commercial one.

The glass tubes are capillaries supporting a pressure up to 300 MPa.[20] The external diameter is standard (5 to 10 mm) but their small internal diameter limits the detection of NMR nuclei with small natural abundance like ^{13}C, ^{15}N or ^{17}O. By replacing the glass with a relatively thin-walled sapphire tube[21] the internal diameter becomes much larger which results in a much better filling factor for the NMR coil. A light weight cylindrically symmetrical titanium valve which dramatically minimizes spinning side bands is shown in Fig. 2.[22,23] Safety considerations are of special importance in the use of this kind of tube, especially when working with gases under pressure. To ensure continuous safety of the user a protective device made of acrylic plastic was developed (Fig. 2). It prevents the user from being exposed directly to the tube while it is being pressurized or under pressure. The maximum working pressure is limited to 10 MPa. The transparent tubes are pressurized outside the NMR magnet and can be easily shaken for rapid dissolution of gases in a liquid.[24] Sapphire tubes are also an ideal tool to measure NMR spectra at temperatures above the boiling point of the solvent used.[22]

To build a special high-pressure high-resolution probe for NMR is a much more demanding task which may explain why only a few research groups have done it so far.[25] The pressure vessels are made from non-magnetic material (such as for example Berylco-25) and contain the high-frequency NMR coil. They allow one to work under non-spinning conditions at pressures typically up to 500 MPa.[26]

A ^{1}H (400 MHz) high-resolution probe for narrow bore (50 mm) cryo-magnets built in our laboratory is shown in Fig. 3.[27] It allows ^{2}H (61.4 MHz) field locking and has a maximum working pressure of 200 MPa. A second, multi-nuclear probe (20 to 160 MHz) for narrow bore (50 mm) cryo-magnets has also been developed in our laboratory. It is equipped with a second electronic circuit for ^{1}H decoupling and ^{2}H (61.4 MHz) field locking. A spectral resolution of less than 1 Hz is typically achieved with these probes (non-spinning).

To study gases dissolved in liquids, the high-pressure probe is equipped with a mixing unit (Fig. 3).[28] This overcomes the very slow diffusion across the gas–liquid interface. With this unit a good mixing is achieved in less than 1 min.[23]

Water exchange from the first coordination shell on metal ions

The replacement of a water molecule from the 1st coordination shell [see eqn. (3)] is an important step in complex formation

$$[M(H_2O)_n]^{z+} + nH_2O^* \rightleftarrows [M(H_2O^*)_n]^{z+} + nH_2O \qquad (3)$$

reactions of metal cations as well as in many redox processes. The general chemistry of aqua ions over the periodic table of elements, its synthesis, structure and reactivity has been reviewed by Richens[29] and the theoretical and experimental aspects of water exchange have been discussed recently in an extensive way.[30] The metal cations are often classified into three groups. The first group is represented by the main group metal ions, varying mainly in ionic radius and electric charge. The number of water molecules in the first coordination sphere

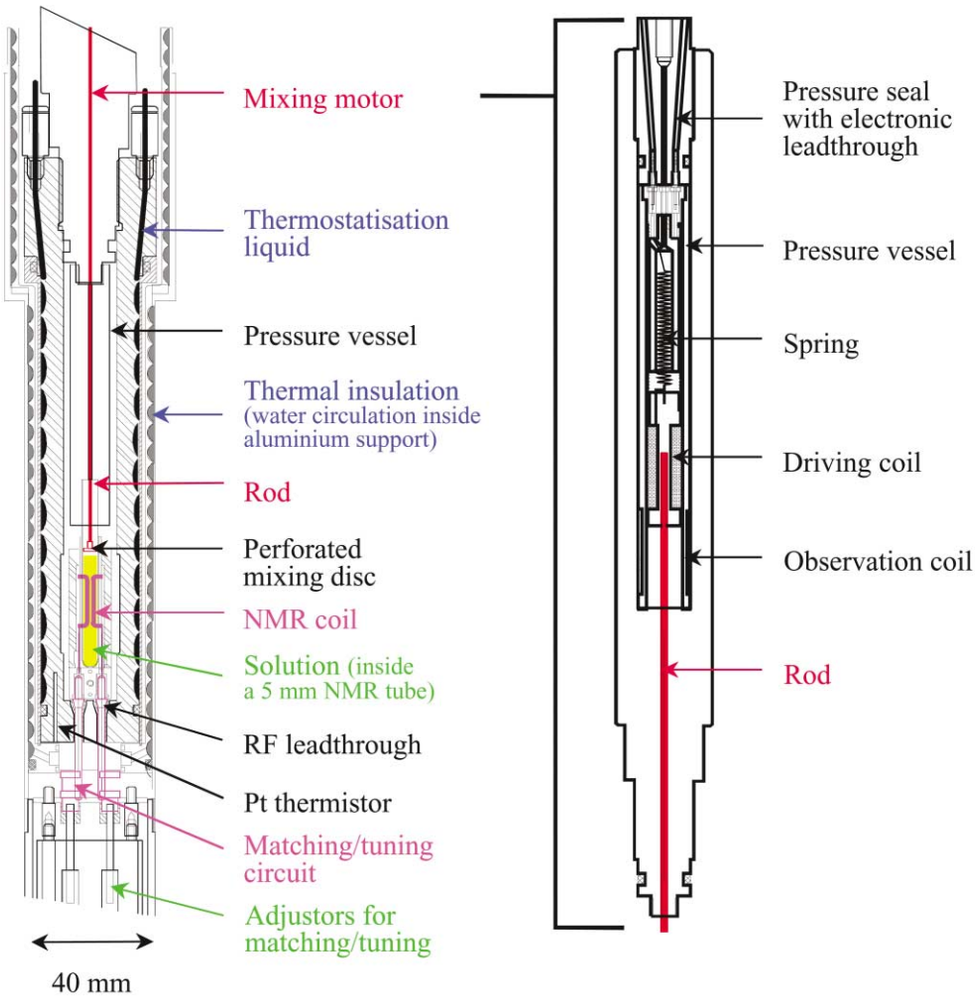

Fig. 3 High-pressure, high-resolution, normal-bore (*Ø* 50 mm) NMR probe (left) equipped with a mixing facility (right) suitable for studies under gas pressures up to 100 MPa. The high-pressure probe can also be used (without the mixer) for studies under liquid pressure to 200 MPa.

spans from 4 to 10 or greater.[31] The second group consists of the d-transition metal ions, which are mainly hexacoordinated with some exceptions like Pd^{2+} and Pt^{2+} which are square planar and Sc^{3+} that might be hepta coordinated.[32] Their exchange rate constants are very strongly linked to the occupancy of their d orbitals. The third group involves the trivalent lanthanide and actinide ions which are eight or nine coordinated. Their kinetic behavior is mostly influenced by the decrease of the ionic radius along the series and the subsequent change in the coordination number.

The observed exchange rate constants cover more than 18 orders of magnitude (Fig. 4) from the most labile monovalent alkaline ions to the very inert trivalent transition metal ions Rh^{3+} and Ir^{3+}. On the slow exchange side, a water molecule stays at room temperature for more than 300 years in the 1st shell of the hexaaqua iridium(III),[22] a third-row transition metal ion with a large ligand field contribution to the activation energy. These extremely slow rates can be determined at high temperature and variable pressure by an isotopical exchange technique using an NMR detection method. On the other extreme, the mean lifetime of a water molecule in the first coordination shell of Cs^+ was estimated to be 200 ps.[33] Cs^+ is the largest monovalent metal cation and has therefore the lowest surface charge density. The most rapid water exchange rate directly measured by ^{17}O NMR ($k_{ex}^{298} = 5.0 \times 10^9\ s^{-1}$ for CN = 7) is that on europium(II).[34] Eu^{2+} is isoelectronic with Gd^{3+} and very similar in size to Sr^{2+} but it is unstable against oxidation in aqueous solution. Because of its size and the 2+ charge Eu^{II} may provide insight as a probe in the chemistry of Ca^{II} and Sr^{II} even if a recent XAFS study on aqueous solutions

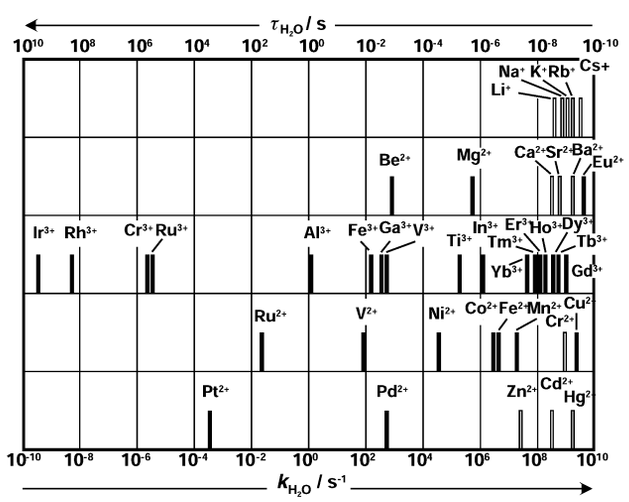

Fig. 4 Mean lifetimes of a single water molecule in the first coordination sphere of a given metal ion, τ_{H_2O}, and the corresponding water exchange rate constants, k_{H_2O}. The full bars indicate directly determined values, and the empty bars indicate values deduced from ligand substitution studies.

of Sr^{2+} and Eu^{2+} surprisingly concluded two different coordination numbers for both ions of 8.0 and 7.2, respectively.[35]

Another very fast exchanging divalent ion, Cu^{II}, has gained some interest recently. It was found from an experimental (neutron diffraction) and theoretical (Car–Parrinello molecular dynamics simulation) study that the copper ion in aqueous

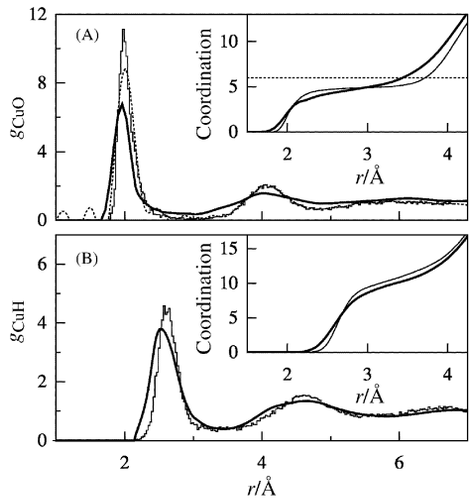

Fig. 5 Partial pair correlation functions $g_{CuO}(r)$ (A) and $g_{CuH}(r)$ (B) obtained by the second-difference isotopic substitution method in neutron diffraction (thick curves) and by first-principles molecular dynamics (thin curves). The dotted curve in (A) corresponds to the theoretical $g_{CuO}(r)$ obtained by considering the same momentum transfer range as in the experiment. The coordination numbers as a function of cutoff radius are given in the insets. The horizontal dashed line (inset, upper panel) corresponds to sixfold oxygen coordination.

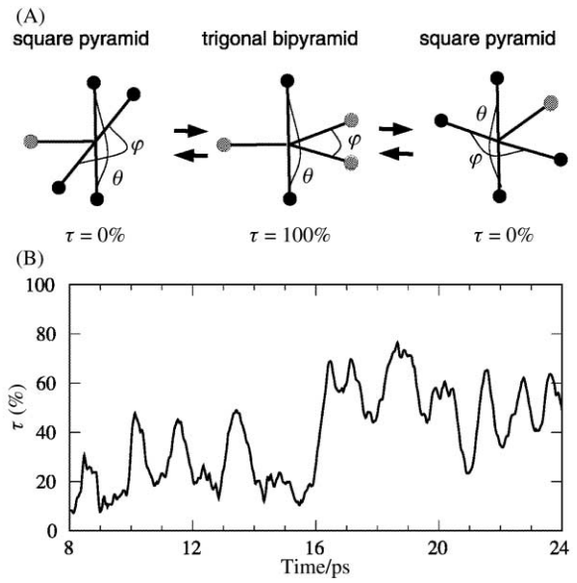

Fig. 6 Time evolution of the coordination geometry of $[Cu(H_2O)_5]^{2+}$: $\tau = (\theta - \varphi)/60 \times 100\%$ where θ and φ are O–Cu–O angles. (A) Berry twist mechanism showing, from left to right, the reorientation of the main axis of a square pyramidal configuration by pseudorotations *via* a trigonal bipyramidal configuration. The grey atoms in the plane of the trigonal bipyramid are all candidates for becoming apical atoms in a square pyramid. (B) Evolution of τ as derived from the first-principles molecular dynamics simulation (window-averaged over an interval of 0.5 ps). The parameter τ describes, in a continuous way, intermediate configurations of the fivefold-coordinated Cu(II) aqua ion ranging between the regular square pyramidal ($\tau = 0\%$) and the regular trigonal bipyramidal ($\tau = 100\%$) configurations.

solution is surrounded by five water molecules (as can be seen from the running coordination number in Fig. 5, inset) arranged in a trigonal bipyramid or in a square pyramid.[36] This is in contrast to what was generally accepted, namely that the Jahn–Teller distorted octahedron, observed in the solid state, is also present in solution. From ^{17}O NMR an inter-conversion rate of 2×10^{11} s^{-1} and a water exchange rate of 4.4×10^9 s^{-1} was obtained using the geometry of hexacoordinated Cu^{2+}.[37] Reanalysing the same NMR relaxation data with a new model including only five H_2O molecules in the first coordination sphere and a similar rapid inter-conversion between the two geometries mentioned above (Fig. 6) yielded a water exchange rate of $(5.7 \pm 0.2) \times 10^9$ s^{-1} slightly enhanced with respect to the value obtained previously assuming sixfold coordination.

Activation volumes for water exchange from the 1st coordination shell of aqua ions are collected in Tables 1 to 4. With the exception of the value for $[Cr(H_2O)_6]^{3+}$ they were all obtained from variable pressure ^{17}O NMR studies. In the following we would like to summarize some general trends for the water exchange mechanism which can be drawn from these $\Delta V^{\ddagger}$.

Diamagnetic metal ions

There are only a few main group metal ions amenable to detailed mechanistic study of water exchange: Be^{2+}, Mg^{2+}, Al^{3+}, Ga^{3+} and In^{3+} (Table 1). They provide the opportunity to study the influence of size and charge on mechanism without the complicating effects of the variation of the electronic occupancy in the d orbitals. The tetrahedrally[8,38] coordinated Be^{II} and the octahedrally[39] coordinated Mg^{II} show relatively slow water exchange rates from the first coordination sphere. The water exchange reaction on $[Be(H_2O)_4]^{2+}$ is characterized by the most negative activation volume observed for a water exchange process ($\Delta V^{\ddagger} = -13.6$ cm^3 mol^{-1}), which is close to a calculated limiting $\Delta V^{\ddagger} = -12.9$ cm^3 mol^{-1} for an A mechanism (hexaaqua ion).[40] The water exchange rate for $[Mg(H_2O)_6]^{2+}$ [41] lies between those of $[Co(H_2O)_6]^{2+}$ and $[Ni(H_2O)_6]^{2+}$ and reflects the order of ionic radii of these three ions (Table 1). The strongly positive activation volume ($\Delta V^{\ddagger} = +6.7$ cm^3 mol^{-1}) is intermediate between those obtained for Co^{2+} and Ni^{2+}. Based on the similarity between Mg^{2+} and these ions an I_d or D mechanism is proposed for H_2O exchange.

The trivalent cations Al^{3+}, Ga^{3+} and In^{3+} have closed shell configurations and differ strongly in their ionic radii (Table 1). Rate constants and activation parameters for water exchange on Al^{III} [42] and Ga^{III} [43] have been determined from kinetic ^{17}O NMR experiments (Table 1). Water exchange processes on $[Al(H_2O)_6]^{3+}$ and $[Ga(H_2O)_6]^{3+}$ are characterized by positive $\Delta V^{\ddagger}$ values. From *ab-initio* calculations it was concluded that the water exchange on Al^{3+} and Ga^{3+} hexaaqua complexes proceeds *via* a D mechanism involving a pentacoordinated intermediate $[M(H_2O)_5 \cdot H_2O]^{3+}$.[44] The calculated activation energies $\Delta E^{\ddagger}$ for these complexes are in remarkable quantitative agreement with the experimental values for $\Delta H^{\ddagger}$. Unfortunately, the water exchange rate on In^{III} is too fast to be measured and only a lower limit could be obtained. The *ab-initio* calculation on aqua ions of In^{3+} gave a much lower energy pathway for an a activated mechanism.[44] Together with the presence of a stable seven-coordinate intermediate an A mechanism was assigned for H_2O exchange at $[In(H_2O)_6]^{3+}$. Activation volumes were estimated from these cluster calculations using the Connolly surface.[45] The corresponding $\Delta V^{\ddagger}$ for an associative exchange process calculated for In^{3+} was -5.2 cm^3 mol^{-1}. The change in mechanism from dissociative (Al^{3+}, Ga^{3+}) to associative (Sc^{3+}, In^{3+}) has already been observed experimentally for organic solvent exchange reactions.[46]

First-row octahedral transition metal ions

Volumes of activation for water exchange on divalent high spin 1st row transition metal ions (Table 2) indicate that the mechanism progressively changes from an associative activation mode for the early elements to a dissociative activation mode for the later ones. This changeover is explained by the progressive filling of the d orbitals and the decrease in ionic radii along the series, both factors disfavouring bonding processes. The activation volume measure for water exchange on copper(II) ($\Delta V^{\ddagger} = 2.0$ cm^3 mol^{-1}) is much smaller than the one measured for nickel(II) ($\Delta V^{\ddagger} = 7.2$ cm^3 mol^{-1}) but still positive. This could effectively reflect the decrease in coordination number from six (Ni^{2+}) to five for Cu^{2+}.

Table 1 Exchange rate constants and activation volumes for exchange on diamagnetic metal ions

Ion	r_i/pm	Geometry	k(298 K)/s^{-1}	$\Delta V^{\ddagger}$/cm^3 mol^{-1}	Mechanism	Ref.
$[Be(H_2O)_4]^{2+}$	27	Tetrahedral	7.3×10^2	−13.6	A	40
$[Mg(H_2O)_6]^{2+}$	72	Octahedral	6.7×10^5	+6.7	I_d, D	41
$[Al(H_2O)_6]^{3+}$	54	Octahedral	1.92	+5.7	D	42
$[Ga(H_2O)_6]^{3+}$	62	Octahedral	4.0×10^2	+5.0	D	43
$[In(H_2O)_6]^{3+}$	80	Octahedral	$>3.0 \times 10^4$	−5.2[a]	A, I_a	44

[a] Estimated from *ab-initio* calculations.

Table 2 Exchange rate constants and activation volumes for water exchange on first row transition metal ions

Ion	r_i/pm	Geometry	k(298 K)/s^{-1}	$\Delta V^{\ddagger}$/cm^3 mol^{-1}	Mechanism	Ref.
$[V(H_2O)_6]^{2+}$	79	Octahedral	8.7×10^1	−4.1	I_a	47
$[Mn(H_2O)_6]^{2+}$	83	Octahedral	2.1×10^7	−5.4	I_a	48
$[Fe(H_2O)_6]^{2+}$	78	Octahedral	4.39×10^6	+3.8	I_d	48
$[Co(H_2O)_6]^{2+}$	74	Octahedral	3.18×10^6	+6.1	I_d	48
$[Ni(H_2O)_6]^{2+}$	69	Octahedral	3.15×10^4	+7.2	I_d	48
$[Cu(H_2O)_5]^{2+}$[a]	73	Trigonal bipyramid, square pyramid	5.7×10^9	+2.0	I_d	36
$[Ti(H_2O)_6]^{3+}$	67	Octahedral	1.8×10^5	−12.1	A, I_a	49
$[V(H_2O)_6]^{3+}$	64	Octahedral	5.0×10^2	−8.9	I_a	50
$[Cr(H_2O)_6]^{3+}$	61	Octahedral	2.4×10^{-6}	−9.6	I_a	51
$[Fe(H_2O)_6]^{3+}$	64	Octahedral	1.6×10^2	−5.4	I_a	52
$[Ga(H_2O)_6]^{3+}$	62	Octahedral	4.0×10^2	+5.0	D	43

[a] Water exchange rate for $[Cu(H_2O)_6]^{2+}$ (distorted octahedron): k(298 K) = 4.4×10^9 (ref. 37)

Table 3 Exchange rate constants and activation volumes for water exchange on second and third row transition metal ions

Ion	r_i/pm	Geometry	k(298 K)/s^{-1}	$\Delta V^{\ddagger}$/cm^3 mol^{-1}	Mechanism	Ref.
$[Ru(H_2O)_6]^{2+}$	73	Octahedral	1.8×10^{-2}	−0.4	I_d	58
$[Pd(H_2O)_6]^{2+}$	64	Square planar	5.6×10^2	−2.2	I_a	59
$[Pt(H_2O)_4]^{2+}$	60	Square planar	3.9×10^{-4}	−4.6	I_a	60
$[Ru(H_2O)_6]^{3+}$	68	Octahedral	3.5×10^{-6}	−8.3	I_a	58
$[Rh(H_2O)_6]^{3+}$	66	Octahedral	2.2×10^{-9}	−4.2	I_a	61
$[Ir(H_2O)_6]^{3+}$	68	Octahedral	1.1×10^{-10}	−5.7	I_a	22

Table 4 Exchange rate constants and activation volumes for water exchange on lanthanide ions

Ion	r_i/pm	Geometry	k(298 K)/s^{-1}	$\Delta V^{\ddagger}$/cm^3 mol^{-1}	Mechanism	Ref.
$[Eu(H_2O)_7]^{2+}$[a]	120	—	5.0×10^9	−11.3	I_a, A	36
$[Gd(H_2O)_8]^{3+}$	105.3	Square-antiprism	1.2×10^9	−3.3	I_a	64, 65
$[Tb(H_2O)_8]^{3+}$	104.0	Square-antiprism	5.6×10^8	−5.7	I_a	64, 65
$[Dy(H_2O)_8]^{3+}$	102.7	Square-antiprism	4.3×10^8	−6.0	I_a	64, 65
$[Ho(H_2O)_8]^{3+}$	101.5	Square-antiprism	2.1×10^8	−6.6	I_a	64, 65
$[Er(H_2O)_8]^{3+}$	100.4	Square-antiprism	1.3×10^8	−6.9	I_a	64, 65
$[Tm(H_2O)_8]^{3+}$	99.4	Square-antiprism	0.9×10^8	−6.0	I_a	64, 65
$[Yb(H_2O)_8]^{3+}$	98.5	Square-antiprism	0.5×10^8		I_a	64, 65

[a] Water exchange rate for $[Eu(H_2O)_8]^{2+}$ (r_i = 125 pm, square-antiprism): k(298 K) = 4.4×10^9 s^{-1} (ref. 65).

For trivalent high spin ions (Table 2) the $\Delta V^{\ddagger}$ values become decreasingly negative on going from Ti^{III} to Fe^{III}, with a positive value for Ga^{III}. This changeover in mechanism from associative to dissociative activation mode is confirmed by the few results available in non-aqueous solvents.[53] In the last few years Rotzinger has published several *ab-initio* calculations on 1st row transition metals.[54] In summary, his results on first row transition metals provided the following picture. Hexacoordinated Sc^{3+}, Ti^{3+} and V^{3+} react *via* an associative A mechanism with relatively long-lived intermediates. The dissociative pathway is the only one possible for water exchange on Ni^{2+}, Cu^{2+} and Zn^{2+}. For the elements in the middle of the 3d series both associative (I_a/A) and dissociative (D) pathways can occur.

Ziegler found from a density functional study[55] on $[Cu(H_2O)_n]^{2+}$ (n = 3–8) that in the case of n = 8 the most favoured structure, has only four water molecules in the first hydration shell, and all four other water molecules are double-hydrogen-bonded to the primary shell water molecules. In this structure the number of hydrogen bonds is maximized with four hydration shell water molecules, and this structure is strongly favoured in terms of energy over other possibilities. This theoretical study clearly shows that for Cu^{2+} hydrogen bond formation between first and second shell water molecules strongly competes with binding of H_2O molecules to the axial position of the Jahn–Teller distorted copper ion. Further calculation with even more than eight water molecules will be

necessary to solve this question definitively. As already mentioned above, from first-principles molecular dynamics (Car–Parrinello MD), where the outer coordination shells are fully taken into account, a coordination with five water molecules was found, in agreement with the experimental data of neutron diffraction.[10]

Second- and third-row octahedral transition metal ions

For the low-spin t_{2g}^6 hexaaqua ions $[Ru(H_2O)_6]^{2+}$, $[Rh(H_2O)_6]^{3+}$ and $[Ir(H_2O)_6]^{3+}$ one would *a priori* predict a dissociative activation mode. The filled t_{2g} orbitals, spread out between ligands, electrostatically disfavour the approach of a seventh molecule towards a face or edge of the octahedron and therefore decrease the ease of bond-making. In a first study of the mechanism of substitution on $[Ru(H_2O)_6]^{2+}$, it was shown that the rate constants for the anation reactions by Cl^-, Br^-, and I^- were very similar, indicating identical steps to reach the transition state (*i.e.* dissociation of H_2O).[56] Later, this study was extended to a large variety of ligands possessing various charges and nucleophilicities, and it was clearly demonstrated that the rate determining step of the monocomplex formation reactions was independent of the nature of the entering ligand. An I_d mechanism was therefore attributed for the substitution reactions on $[Ru(H_2O)_6]^{2+}$.[57] However, a variable pressure study of water exchange on this ion gave an activation volume close to zero ($\Delta V^{\ddagger} = -0.4$ cm^3 mol^{-1}) and was therefore interpreted as an interchange I mechanism without predominant "a" or "d" character (Table 3).[58] Attempts to compute, at the restricted Hartree–Fock (SCF) level using the self-consistent reaction field model (SCRF), a transition state for an I mechanism failed and only a D mechanism with a five coordinate intermediate could be computed.[62] The impossibility of calculating a transition state for the I_d mechanism does not mean that it does not exist: it is just not available within the model in which the second coordination sphere is not treated quantum chemically. Therefore, the experimental together with theoretical results available today suggest that water exchange on $[Ru(H_2O)_6]^{2+}$ proceeds *via* a "d activation", either the I_d or D mechanism. This is also in agreement with the high pressure study of the formation of $[Ru(H_2O)_5(DMF)]^{2+}$ from the aqua ion, for which the volume of the transition state lies between the volume of the reactant and the volume of the products and where an I_d mechanism has been assigned.[63]

$[Rh(H_2O)_6]^{3+}$ and its third-row analog $[Ir(H_2O)_6]^{3+}$ are the most inert aqua ions known to date. The lifetime of a water molecule in the first coordination shell of Ir^{3+} is 9.1×10^9 s (at 298 K), which corresponds to about 300 years. The negative activation volumes of the Rh^{3+} and Ir^{3+} ions suggest the operation of associative I_a exchange mechanisms (Table 3). Theoretical calculations have allowed characterization of the seven-coordinate transition state $\{[Rh(OH_2)_5 \cdots (OH_2)_2]^{3+}\}^{\ddagger}$ corresponding to the I_a exchange mechanism for rhodium.[62] Why do Rh^{3+} and Ru^{2+} undergo water exchange *via* disparate mechanisms although they are isoelectronic? The charges are different effecting especially the M–O bond strength. This is manifested by the calculated activation energies for the exchange reactions *via* the D mechanism: 71.9 kJ mol^{-1} for Ru^{2+} and 136.6 kJ mol^{-1} for Rh^{3+} [62] (Fig. 7). Therefore, the strong Rh^{III}–O bonds allow the water exchange on $[Rh(H_2O)_6]^{3+}$ to proceed *via* the I_a pathway, whereas the same reaction on $[Ru(H_2O)_6]^{2+}$, which has considerably weaker Ru^{II}–O bonds, follows I_d or D mechanisms. The low-spin t_{2g}^5 $[Ru(H_2O)_6]^{3+}$ is four orders of magnitude more labile than the t_{2g}^6 $[Ru(H_2O)_6]^{2+}$ [58] and, according to the same arguments developed above, exchanges water by an I_a mechanism. The knowledge of the difference in lability of $[Ru(H_2O)_6]^{2+}$ and $[Ru(H_2O)_6]^{3+}$ led to the unequivocal identification of an outer-sphere mechanism operating in the electron exchange between these two aqua complexes.[58]

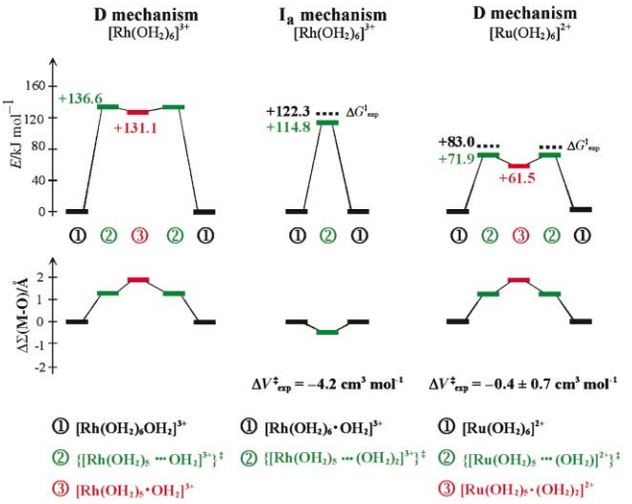

Fig. 7 Energies calculated with a polarizable continuum model, differences of the sums of all metal–oxygen bond lengths, ΔΣ(M–O), and energy profiles for water exchange on rhodium(III) (left and middle) and ruthenium(II) (right) hexaaqua ions.

Lanthanide ions

The only trivalent lanthanides which could be studied are the heavier, paramagnetic ions from Gd^{3+} to Yb^{3+}. These are all eight coordinate in contrast to the ions of the light elements. The water exchange rates measured by ^{17}O NMR are closely correlated with the rate of the interchange between an inner sphere water molecule and a SO_4^{2-} anion from the outer sphere coordination.[64] The values show a maximum in the middle of the series, corresponding to the crossover region in CN from nine to eight. The activation volumes measured are all negative,[65] indicating an associatively activated water exchange mechanism (Table 4). This observation can be explained in terms of the coordination equilibrium observed in the middle of the series. For the heavy lanthanides, the octa ion is the lowest energy species and the ennea aqua ion represents the intermediate (or transition state) in the associatively activated water exchange reaction. The exchange rates become faster towards the middle of the series as the difference in the energy between octa aqua and ennea aqua ions decreases. For the mid-series lanthanides, the octa and the ennea aqua species are in equilibrium. The transition from one species to the other requires relatively little energy, so that these lanthanides should have the fastest water exchange rates of the series. For the light lanthanides, the ennea aqua ion is now the lowest energy species. One can expect, therefore, that the octa aqua ion will be the intermediate (or transition state) in the exchange process, which will proceed *via* a dissociatively activated mechanism. One would expect to observe an increase in water exchange rates and positive activation volumes from La^{3+} to Nd^{3+}. Unfortunately, so far it has not proved possible to demonstrate experimentally these predictions for the light lanthanide ions. The absence of significant crystal field splitting and the shielding of the f orbitals makes classical molecular dynamics simulations feasible. Structural and dynamic results of MD simulations of an early (Nd^{3+}), a middle (Sm^{3+}) and a heavy (Yb^{3+}) lanthanide are in good agreement with experimental findings.[30,36]

Complex formation of Ru(II) aqua complexes with small gaseous molecules

Shortly after the publication of the first facile synthesis of $[Ru(H_2O)_6](tos)_2$ (tos = tosylate),[67] a very interesting and promising chemistry has started on the organometallic chemistry of Ru(II) in water. For example, $[Ru(H_2O)_6](tos)_2$, was

Table 5 Experimental free energies of activation, $\Delta G^{\ddagger}$ (298.15 K), for water exchange, calculated binding energies, E_b, and bond distances, d, for $[Ru(H_2O)_5L]^{2+}$ complexes (L = H_2O, $H_2C{=}CH_2$, CO, N_2)

$[Ru(H_2O)_5L]^{2+}$	Ru–H_2O_{ax} bond			Ru–L bond
L	E_b/kJ mol^{-1}	$\Delta G^{\ddagger}$/kJ mol^{-1}	d/Å	E_b/kJ mol^{-1}
$H_2C{=}CH_2$	166.2	70.4	2.188	248.6
H_2O	179.4	83.0	2.095	179.4
CO	182.5	81.0	2.151	286.4
N_2	208.5	99.1	2.090	188.3

shown to be an ideal starting material for the straightforward syntheses of $[Ru(H_2O)_5L]^{2+}$ (L = N_2,[68] CO,[69] $H_2C{=}CH_2$[70]). The reaction [eqn. (4)] was followed as a function of temperature

$$[Ru(H_2O)_6]^{2+} + L \longrightarrow [Ru(H_2O)_5L]^{2+} + H_2O \qquad (4)$$

and concentration, which means gas pressure, using the high-pressure probe described above.[71]

The water exchange reactions on the reactants and products have been followed by ^{17}O NMR spectroscopy. The variable-pressure and variable-temperature kinetic studies made on selected examples are all in accordance with a dissociative activation mode for water exchange. The positive activation volumes obtained for the axial and equatorial water exchange reactions on $[Ru(H_2O)_5(H_2C{=}CH_2)]^{2+}$ ($\Delta V_{ax}^{\ddagger}$ and $\Delta V_{eq}^{\ddagger} = +6.5$ and $+6.1$ cm^3 mol^{-1}) are the strongest evidence of this conclusion. The increasing *cis*-effect series was established according to the lability of the equatorial water molecules and is as follows: $F_2C{=}CH_2 \cong CO < Me_2SO < N_2 < H_2C{=}CH_2 < MeCN < H_2O$. The increasing *trans*-effect series, established from the lability of the axial water molecule, is the following: $N_2 \ll MeCN < H_2O < CO < Me_2SO < H_2C{=}CH_2 < F_2C{=}CH_2$. Density functional calculations showed a variation of the Ru–H_2O_{ax} bond length (Table 5). The best correlation was found between the lability and the calculated Ru–H_2O_{ax} bond energies. From the DFT calculations it appears that a decrease of the electronic density along the Ru–O_{ax} bond and the increase of the lability can be related to an increase of the π-accepting capability of the ligand. In an experimental study with L = $H_2C{=}CH_2$, CH_3CN, $(CH_3)_2SO$ and CO is was found that the rate determining step in the exchange of L on $[Ru(H_2O)_5L]^{2+}$ is the rupture of the Ru–H_2O_{ax} bond with *trans*-$[Ru(H_2O)_4L_2]^{2+}$ as reaction intermediate.[72] Due to the *trans* effect exercised by these strong π-accepting ligands, the ligand exchange reaction is faster than the mono-complex formation reactions. In the *cis*-bis-complex formation Ru–H_2O_{eq} bond breaking is also the rate determining step, but due to the decrease in lability of the water molecules *cis* to π-accepting ligands, these reactions are much slower. As a general rule, the rate of these complex formation reactions, of a dissociative nature, can be predicted from the water exchange rates determined by ^{17}O NMR.

Summary and outlook

The results presented in this perspective demonstrate the usefulness of pressure variation for the elucidation of mechanisms of solvent exchange reactions on metal ions. Even if the distinction between a limiting and an interchange mechanism, based on the magnitude of the activation volumes, is not straight forward, the activation mode, associative or dissociative, can mostly be assigned unambiguously from the sign of $\Delta V^{\ddagger}$. Different nuclear magnetic resonance techniques have to be applied to measure water exchange rate constants on metal ions over a range of more than 18 orders of magnitude. High-pressure equipment, such as high-pressure NMR probes, is still not easy to obtain.

The use of quantum mechanical calculations has also become a valuable tool in studies of solvent exchange reactions. These calculations can be performed on the ground state and on transition states or intermediates with increased or decreased coordination number. They are useful for distinguishing between possible pathways and/or to give insight on the mechanism, not available experimentally. The results obtained also show that the influence of the second coordination sphere on the structure and the energies can be important especially if the first coordination sphere is very labile. A very promising computational technique which includes outer sphere effects is Car–Parrinello molecular dynamics (first-principles MD). This method is limited, with actually available computers, to the simulation of very fast (some pico-seconds) processes in solution.

Acknowledgements

The authors gratefully acknowledge financial support from the Swiss National Science Foundation and the Swiss Office for Education and Science (COST Program). Furthermore, we wish to thank the large number of people who have contributed to the work performed in Lausanne.

References

1 R. van Eldik, *Inorganic High Pressure Chemistry: Kinetics and Mechanisms*, Elsevier, Amsterdam, 1986.
2 H. R. Hunt and H. Taube, *J. Am. Chem. Soc.*, 1958, **80**, 2642.
3 K. Heremans, J. Snauwaert and J Rijkenberg, in *High Pressure Science and Technology* ed. K. D. Timmerhaus and M. S. Berber, Plenum, New York, vol. 1, 1979.
4 E. F. Caldin, M. W. Grant and B. B. Hasinoff, *J. Chem. Soc., Faraday Trans. 1*, 1972, **68**, 2247.
5 K. R. Brower, *J. Am. Chem. Soc.*, 1968, **90**, 5401.
6 H. Vanni and A. E. Merbach, *J. Magn. Reson.*, 1978, **29**, 11.
7 R. Car and M. Parrinello, *Phys. Rev. Lett.*, 1985, **55**, 2471.
8 D. Marx, M. Sprik and M. Parrinello, *Chem. Phys. Lett.*, 1997, **273**, 360.
9 L. M. Ramaniah, M. Bernasconi and M. Parrinello, *J. Chem. Phys.*, 1999, **111**, 1587.
10 A. Pasquarello, I. Petri, P. S. Salmon, O. Parisel, R. Car, E. Tóh, D. H. Powell, H. E. Fischer, L. Helm and A. E. Merbach, *Science*, 2001, **291**, 856.
11 C. H. Langford and H. B. Gray, *Ligand Substitution Processes*, W. A. Benjamin Inc., New York, 1965.
12 A. E. Merbach, *Pure Appl. Chem.*, 1982, **54**, 1479; A. E. Merbach, *Pure Appl. Chem.*, 1987, **59**, 161.
13 T. W. Swaddle, *Commun. Inorg. Chem.*, 1991, **12**, 237.
14 R. E. Connick and B. J. Alder, *J. Phys. Chem.*, 1983, **87**, 2764.
15 R. van Eldik, *Pure Appl. Chem.*, 1992, **64**, 1439; R. van Eldik and A. E. Merbach, *Commun. Inorg. Chem.*, 1992, **12**, 341.
16 T. W. Swaddle and M. K. S. Mak, *Can. J. Chem.*, 1983, **61**, 473; T. W. Swaddle, *Adv. Inorg. Bioinorg. Mech.*, 1983, **2**, 95.
17 R. D. Shannon, *Acta Crystallogr., Sect. A*, 1976, **32**, 751.
18 G. B. Benedek and E. M. Purcell, *J. Chem. Phys.*, 1954, **22**, 2003.
19 L. Helm, D. H. Powell and A. E. Merbach, in *High-Pressure Techniques in Chemistry and Physics: A Practical Approach*, ed. W. Holzapfel and N. Isaacs, Oxford University Press, Oxford, UK, 1997.
20 E. W. Lang and H. D. Lüdemann, *NMR*, 1991, **24**, 129; H. Yamada, *NMR*, 1991, **24**, 233.
21 D. C. Roe, *J. Magn. Reson.*, 1985, **63**, 388; I. T. Horwath and E. E. Ponce, *Rev. Sci. Instrum.*, 1991, **62**, 1104.
22 A. Cusanelli, U. Frey, D. T. Richens and A. E. Merbach, *J. Am. Chem. Soc.*, 1996, **118**, 5265.
23 A. Cusanelli, U. Frey, D. Marek and A. E. Merbach, *Spectrosc. Eur.*, 1997, **9**, 22.

24 R. Churlaud, Ph.D. Thesis, University of Lausanne, 1999.
25 A. E. Merbach and H. Vanni, *Proc. XVIIIth Int. Conf. Coord. Chem.*, 1976, 269; D. L. Pisanello, L. Helm, P. Meier and A. E. Merbach, *J. Am. Chem. Soc.*, 1983, **105**, 4528; D. G. Van der Velde and J. Jonas, *J. Magn. Reson.*, 1987, **71**, 480; U. Frey, L. Helm and A. E. Merbach, *High Pressure Res.*, 1990, **2**, 237; B. Moullet, U. Frey, L. Helm, T. Tschanz, A. E. Merbach and R. Ith, *High Pressure Res.*, 1994, **12**, 285; A. Zahl, A. Neubrand, S. Aygen and R. van Eldik, *Rev. Sci. Instrum.*, 1994, **65**, 882; M. Schick, Thesis, ETH Zürich, 1998.
26 J. Jonas, *NMR*, 1991, **24**, 85.
27 A. Cusanelli, L. Nicula-Dadci, U. Frey and A. E. Merbach, *Inorg. Chem.*, 1997, **36**, 2211.
28 P. Favre, U. Frey, D. Marek and F. Metz, *US Patent*, 5 545 998, 1996.
29 D. T. Richens, *The Chemistry of Aqua Ions*, Wiley, Chichester, 1997.
30 L. Helm and A. E. Merbach, *Coord. Chem. Rev.*, 1999, **187**, 151.
31 H. Ohtaki and T. Radnai, *Chem. Rev.*, 1993, **93**, 1157.
32 P. Smirnov, H. Wakita and T. Yamaguchi, *J. Phys. Chem. B*, 1998, **102**, 4802.
33 M. Eigen, *Pure Appl. Chem.*, 1963, **6**, 97; M. Eigen and R. G. Wilkins, *Adv. Chem. Ser.*, 1965, **49**, 55.
34 P. Caravan and A. E. Merbach, *Chem. Commun.*, 1997, 2147; P. Caravan, E. Tóth, A. Rockenbauer and A. E. Merbach, *J. Am. Chem. Soc.*, 1999, **121**, 10403.
35 G. Moreau, L. Helm, J. Purans and A. E. Merbach, submitted.
36 A. Pasquarello, I. Petri, P. S. Salmon, O. Parisel, R. Car, E. Toth, D. H. Powell, H. E. Fischer, L. Helm and A. E. Merbach, *Science*, 2001, **291**, 856.
37 D. H. Powell, L. Helm and A. E. Merbach, *J. Chem. Phys.*, 1991, **95**, 9258.
38 J. Frahm and H.-H. Füdner, *Ber. Bunsen-Ges. Phys. Chem.*, 1980, **84**, 173; T. Yamagushi, H. Ohtaki, E. Spohr, E. Pálinkás, K. Heinzinger and M. M. Probst, *Z. Naturforsch., Teil A*, 1986, **41**, 1175.
39 N. Matwiyoff and H. Taube, *J. Am. Chem. Soc.*, 1968, **90**, 2796; A. Fratiello, R. R. Lee, V. M. Nishida and R. E. Schuster, *J. Chem. Phys.*, 1968, **48**, 3705; J. Jorgin, P. S. Knapp, W. L. Flint, G. Highberger and E. R. Malinowsky, *J. Chem. Phys.*, 1971, **54**, 178; R. Caminiti, G. Licheri, G. Piccaluga and G. Pinna, *J. Appl. Crystallogr.*, 1979, **12**, 34; R. Caminiti, G. Cerioni, G. Crisponi and P. Cucca, *Z. Naturforsch., Teil A*, 1988, **43**, 317.
40 P.-A. Pittet, G. Elbaze, L. Helm and A. E. Merbach, *Inorg. Chem.*, 1990, **29**, 1936.
41 A. Bleuzen, P.-A. Pittet, L. Helm and A. E. Merbach, *Magn. Reson. Chem.*, 1997, **35**, 765.
42 D. Hugi-Cleary, L. Helm and A. E. Merbach, *Helv. Chim. Acta*, 1985, **68**, 545.
43 D. Fiat and R. E. Connick, *J. Am. Chem. Soc.*, 1968, **90**, 608; D. Hugi-Cleary, L. Helm and A. E. Merbach, *J. Am. Chem. Soc.*, 1987, **109**, 4444.
44 Th. Kowall, P. Caravan, H. Bourgeois, L. Helm, F. P. Rotzinger and A. E. Merbach, *J. Am. Chem. Soc.*, 1998, **120**, 6569.
45 M. L. Connolly, *Science*, 1983, **221**, 709.
46 S. F. Lincoln and A. E. Merbach, *Adv. Inorg. Bioinorg. Mech.*, 1983, **2**, 95.
47 Y. Ducommun, D. Zbinden and A. E. Merbach, *Helv. Chim. Acta*, 1982, **65**, 1385.
48 Y. Ducommun, K. Newman and A. E. Merbach, *Inorg. Chem.*, 1980, **19**, 3696.
49 A. D. Hugi, L. Helm and A. E. Merbach, *Inorg. Chem.*, 1987, **26**, 1763.
50 A. D. Hugi, L. Helm and A. E. Merbach, *Helv. Chim. Acta*, 1985, **68**, 508.
51 F.-C. Xu, H. R. Krouse and T. W. Swaddle, *Inorg. Chem.*, 1985, **24**, 267.
52 T. W. Swaddle and E. E. Merbach, *Inorg. Chem.*, 1981, **20**, 4212.
53 A. E. Merbach and J. W. Akitt, *NMR*, 1990, **24**, 191.
54 F. P. Rotzinger, *J. Am. Chem. Soc.*, 1996, **118**, 6760; F. P. Rotzinger, *J. Am. Chem. Soc.*, 1997, **119**, 5230; F. Rotzinger, *Helv. Chim. Acta*, 2000, **83**, 3006.
55 A. Bérces, T. Nukada, P. Margl and T. Ziegler, *J. Phys. Chem. A*, 1999, **103**, 9693.
56 T. W. Kallen and J. E. Earley, *Inorg. Chem.*, 1971, **10**, 1149.
57 N. Aebischer, G. Laurenczy, A. Ludi and A. E. Merbach, *Inorg. Chem.*, 1993, **32**, 2810.
58 I. Rapaport, L. Helm, A. E. Merbach, P. Bernhard and A. Ludi, *Inorg. Chem.*, 1988, **27**, 873.
59 L. Helm, L. I. Elding and A. E. Merbach, *Helv. Chim. Acta*, 1984, **67**, 1453.
60 L. Helm, L. I. Elding and A. E. Merbach, *Inorg. Chem.*, 1985, **24**, 1718.
61 G. Laurenczy, I. Rapaport, D. Zbinden and A. E. Merbach, *Magn. Reson. Chem.*, 1991, **29**, 45.
62 D. De Vito, H. Sidorenkova, F. P. Rotzinger, J. Weber and A. E. Merbach, *Inorg. Chem.*, 2000, **39**, 5547.
63 N. Aebischer and A. E. Merbach, *Inorg. React. Mech.*, 1999, **1**, 233.
64 C. Cossy, L. Helm and A. E. Merbach, *Inorg. Chem.*, 1988, **27**, 1973; D. P. Fay, D. Litchinsky and N. Purdie, *J. Phys. Chem.*, 1969, **73**, 544.
65 C. Cossy, L. Helm and A. E. Merbach, *Inorg. Chem.*, 1989, **28**, 2699.
66 T. Kowall, F. Foglia, L. Helm and A. E. Merbach, *J. Am. Chem. Soc.*, 1995, **117**, 3790; T. Kowall, F. Foglia, L. Helm and A. E. Merbach, *J. Phys. Chem.*, 1995, **99**, 13078; Th. Kowall, F. Foglia, L. Helm and A. E. Merbach, *Eur. Chem. J.*, 1996, **2**, 285.
67 P. Bernhard, H.-B. Bürgi, J. Hauser, H. Lehmann and A. Ludi, *Inorg. Chem.*, 1982, **21**, 3936.
68 G. Laurenczy, L. Helm, A. Ludi and A. E. Merbach, *Inorg. Chim. Acta*, 1991, **189**, 131.
69 G. Laurenczy, L. Helm, A. Ludi and A. E. Merbach, *Helv. Chim. Acta*, 1991, **74**, 1236.
70 G. Laurenczy and A. E. Merbach, *J. Chem. Soc., Chem. Commun.*, 1993, 187.
71 N. Aebischer, E. Sidorenkova, M. Ravera, G. Laurenczy, D. Osella, J. Wber and A. E. Merbach, *Inorg. Chem.*, 1997, **36**, 6009.
72 N. Aebischer, R. Churlaud, L. Dolci, U. Frey and A. E. Merbach, *Inorg. Chem.*, 1998, **37**, 5915.